Do observations on surface coverage-reactivity correlations always describe the true catalytic process? A case study on ceria

Ramzi Farra,[a] Maik Eichelbaum,[a] Robert Schlögl,[a] László Szentmiklósi,[b] Timm Schmidt,[c] Amol P. Amrute,[d] Cecilia Mondelli,[d] Javier Pérez-Ramírez,[d] Detre Teschner[a,b*]

[a] Fritz-Haber-Institut der Max-Planck Gesellschaft, Faradayweg 4-6, D-14195 Berlin, Germany

[b] Centre for Energy Research, Hungarian Academy of Sciences, Budapest, H-1525, Hungary

[c] Bayer MaterialScience AG, PUR-PTI-PRI, Chempark B598, D-41538 Dormagen, Germany

[d] Institute for Chemical and Bioengineering, Department of Chemical and Applied Biosciences, ETH Zurich, Wolfgang-Pauli-Strasse 10, CH-8093 Zurich, Switzerland

Email: teschner@fhi-berlin.mpg.de

Tel: +49 30 84135408

Fax: +49 30 84134676

Abstract

In situ (*operando*) investigations aim at establishing structure-function and/or coverage-reactivity correlations. Herein, we investigated the HCl oxidation reaction ($4HCl + O_2 \rightarrow 2Cl_2 + 2H_2O$) over ceria. In spite of its remarkable performance, under low oxygen over-stoichiometry this oxide is prone to a certain extent to subsurface/bulk chlorination, which leads to deactivation. *In situ* Prompt Gamma Activation Analysis (PGAA) studies evidenced that the chlorination rate is independent of the pre-chlorination degree but increases at lower oxygen over-stoichiometry, while dechlorination is effective in oxygen-rich feeds and its rate is higher for a more extensively pre-chlorinated ceria. Even bulk $CeCl_3$ could be transformed into CeO_2 under oxygen excess. Electron Paramagnetic Resonance experiments strongly suggested that oxygen activation is inhibited by a high surface chlorination degree. The coverages of most abundant surface intermediates, OH and Cl, were monitored by *in situ* infrared spectroscopy and PGAA under various conditions. Higher temperature and $p(O_2)$ led to enhanced OH coverage, reduced Cl coverage, and increasing reactivity. Variation of p(HCl) gave rise to opposite correlations, while raising $p(Cl_2)$ did not induce any measurable increase in the Cl coverage despite the strong inhibition of the reaction rate. The results indicate that only a small fraction of surface sites are actively involved in the reaction and most of the surface species probed in the *in situ* observation are spectator. Therefore, when performing *in situ* steady-state experiments, a large set of variables should be considered to obtain accurate conclusions.

***Keywords*:** CeO_2, *in situ* FTIR, *in situ* PGAA, EPR, HCl oxidation, surface coverage

Introduction

Heterogeneous catalysis is a kinetically-driven phenomenon, and the reaction rate is proportional to the coverage of *at least one* reactant, or surface species or by the number of free sites. Nevertheless, the dependence can be fairly complex, and the extent of sites occupied by blocking species crucially affects the catalyst's efficiency. The coverage of reactants, intermediates, and products strongly depends on their heat of adsorption at the relevant active surface site and on the barriers related to the formation and elimination of these surface species. The quantitative information on the surface coverage plays an important role in identifying reaction mechanisms, designing alternative catalysts, or validating purely computational approaches. Thus, the knowledge of the surface coverage at meaningful catalytic turnover is critical and has always been the motivation of extensive experimental efforts.[1,2,3] Unfortunately, only a very few number of experimental techniques are capable of deriving such information, the most important ones being the various forms of vibrational spectroscopies. In this manuscript we will experimentally assess the coverage of surface species under catalytic turnover and correlate these with the reactivity. The catalytic HCl oxidation (Deacon reaction) over bulk ceria will serve as our example.

The heterogeneously catalyzed HCl oxidation is a sustainable route to manufacture chlorine, and the current technology is based on RuO_2 catalysts.[4,5,6,7,8] CeO_2 was recently identified as a cheaper potential alternative active phase in view of its remarkable stability, though it requires higher operating temperatures.[9] As revealed by XRD and XPS analyses, when using an appropriate over-stoichiometry of oxygen in the feed gas (O_2:HCl > 0.75) the bulk of ceria was unaffected and only the surface got chlorinated under reaction condition. The mechanism of HCl oxidation over CeO_2 was suggested to involve the following elementary steps: (i) hydrogen abstraction from HCl by basic surface O atoms to form hydroxyl groups leaving chlorine atoms on the surface, (ii) reaction of the hydroxyl groups

with new incoming HCl molecules and/or hydroxyl group recombination on the surface to form water, (iii) water desorption, (iv) re-oxidation of the surface via dissociative adsorption of O_2, and (v) recombination of chlorine atoms evolving in the gas phase as Cl_2.[9] Several of these steps rely on the existence of anionic oxygen vacancies that accommodate dissociated reactants. Based on the above mechanism, adsorbed Cl, OH, and H_2O are the major species populating the surface. These may occupy coordinatively unsaturated cationic sites or lattice O sites by replacement.

This manuscript attempts to address two novel aspects of the Deacon reaction over CeO_2. First, we investigate the chlorine uptake under reaction conditions and follow the kinetics of the dynamic chlorination and dechlorination process depending on the oxygen over-stoichiometry of the feed mixture. Second, we examine the coverage of Cl and OH under various reaction conditions and relate them with reactivity. We show how convincing coverage-rate correlations break down when product inhibition is included in the experiments, and conclude that the observed correlations are associated with the main part of the surface bearing little relevance for the reactivity.

Experimental

Catalysts

$CeCl_3$ (Alfa Aesar, ultra dry, 99.9%) was used as received. CeO_2 (Aldrich, nanopowder, 544841) was calcined in static air at 1173 K for 5 h prior to use. This sample is referred to as CeO_2-A. CeO_2-R was synthesized by thermal decomposition of cerium(III) nitrate hexahydrate (Aldrich, 99.99%) in air by ramping to 1173 K (2 K min^{-1}) and holding for 3 h. CeO_2-A and CeO_2-R possessed BET surface areas of 21 and 5 m^2 g^{-1}, respectively, after catalytic testing. For the EPR experiments, CeO_2-A was treated in O_2:HCl = 0.75 at 703 K for 3 h. This sample is denoted as CeO_2-D.

Basic characterization

Powder X-ray diffraction (XRD) was measured in a PANanalytical X'Pert PRO-MPD diffractometer. Data were recorded in the 10-70° 2θ range with an angular step size of 0.017° and a counting time of 0.26 s per step. N_2 sorption at 77 K was measured in a Quantachrome Quadrasorb-SI gas adsorption analyzer. The samples were degassed in vacuum at 473 K for 12 h prior to the measurement.

In situ Prompt Gamma Activation Analysis (PGAA)

In situ PGAA[10] was utilized to measure the Cl uptake of ceria during HCl oxidation. The technique is based on the detection of element-specific gamma rays emitted upon the capture of neutrons by the nucleus. The investigated volume, in our case a tubular micro-reactor (catalyst bed volume ~ 0.3 cm^3), was probed and the amounts of Cl and Ce were quantified. PGAA was carried out under atmospheric pressure condition at the cold neutron beam of the Budapest Neutron Centre. A Compton-suppressed high-purity germanium crystal was used to detect the prompt gamma photons. Molar ratios (Cl:Ce) were determined from the characteristic peak areas corrected by the detector efficiency and the nuclear data of the observed elements. The gas-phase Cl signal (HCl, Cl_2) was subtracted, thus, all Cl:Ce ratios reported here correspond only to the catalyst itself. The quartz reactor (i.d. = 8 mm) was placed into the neutron beam and surrounded by a specially designed oven having openings for the incoming and outgoing neutrons and for the emitted gamma rays towards the detector. These openings were covered by thin aluminum foils to minimize heat losses. Two CeO_2 materials (CeO_2-A, CeO_2-R) were investigated. As both revealed the same trends, only the more detailed investigation on CeO_2-R is presented in the PGAA section, while results on CeO_2-A are collected in the Electronic Supplementary Information (ESI). 0.8 g of CeO_2-R (sieve fraction 0.1-0.32 mm) was loaded into the reactor. The reaction feed, at a constant total flow of 166.6 cm^3 STP min^{-1}, was supplied by mass flow controllers, and employed HCl

(4.5), O_2 (5.0) N_2 (5.0) and Cl_2 (4.0). Various feed compositions, $p(O_2)$, p(HCl) and $p(Cl_2)$, and reaction temperature were investigated. Details are provided at the appropriate sections. The Cl_2 production was monitored by iodometric titration. The percentage of HCl conversion was determined as X_{HCl} = (2 × mole Cl_2 at the reactor outlet/mole HCl at the reactor inlet) × 100. Further details to PGAA and representative spectra are provided in the ESI.

Catalytic evaluation

The gas-phase oxidation of hydrogen chloride was studied at ambient pressure in a set up described elsewhere.[11] The catalyst (sieve fraction = 0.4-0.6 mm) was loaded in the tubular reactor (8 mm i.d.) and pre-treated in N_2 at 703 K for 30 min. Thereafter, the reaction gases were introduced at a total flow of 166 cm^3 STP min^{-1}. $CeCl_3$ was tested at 703 K or 723 K, O_2:HCl = 2, 4, or 9, and a catalyst weight of 0.5 g. Separated 5 h tests were carried out with fresh loads of $CeCl_3$ for each different O_2:HCl ratio and temperature. Used samples were collected for *post mortem* characterization after rapidly cooling down the reactor to room temperature in a flow of N_2. Activity data were collected for CeO_2-A after 1 h on stream under all conditions applied to $CeCl_3$ to serve as reference. The influence of Cl_2 co-feeding on the rate of HCl oxidation over CeO_2-A was studied by introducing fixed amounts (2, 3, 4, and 5 cm^3 STP min^{-1}) of Cl_2 to the inlet feed at 703 K and O_2:HCl = 9 (notice HCl flow is 16.6 cm^3 STP min^{-1}), over 0.25 g of catalyst. Data was taken after 1.5 h on stream under each condition. Cl_2 quantification and calculation of the HCl conversion were performed as described in the above section.

In situ Fourier Transform Infrared Spectroscopy (FTIR)

A specially designed home-made cell was used to investigate Deacon catalysts under reaction conditions. Further details about the cell were reported elsewhere.[12] For *in situ* FTIR experiments, 42 mg CeO_2-A was pressed into a self-supporting disc (31.8 mg cm^{-2}). The sample was placed in the sample holder which serves as an internal furnace as well. The pellet

was pre-treated *in situ* by heating it in synthetic air up to 723 K (10 K min^{-1}). Spectra were recorded with a Varian-670 FTIR spectrometer (resolution = 4 cm^{-1}). In most cases, 512 scans were averaged to achieve a satisfactory signal-to-noise ratio. Mass flow controllers were used to supply the reaction feed (total flow = 100 cm^3 STP min^{-1}). The effect of $p(O_2)$, p(HCl), and temperature were investigated under Deacon conditions. In the O_2 partial pressure dependent series, the HCl flow was kept constant at 10 cm^3 STP min^{-1} and $p(O_2)$ was varied to give the following feed composition sequence O_2:HCl:N_2 = 9:1:0, 4:1:5, 2:1:7, 1:1:8 and 0.5:1:8.5. During the measurement of the HCl partial pressure dependence, the O_2 flow was kept constant at 20 cm^3 STP min^{-1} and HCl flow was varied as follows: 10, 6, 3 and 1 cm^3 STP min^{-1}. In the partial pressure variation experiments, the temperature was kept at 703 K. The temperature dependence was investigated by reducing the temperature stepwise, 20 K per step, between 703 and 623 K using a feed composition of O_2:HCl:N_2 = 9:1:0.

Electron Paramagnetic Resonance (EPR) experiments

The X-band EPR experiments were performed in vacuum ($1 \cdot 10^{-4}$ -$8 \cdot 10^{-5}$ mbar) at 77 K on a Bruker ESP 300E spectrometer equipped with the microwave bridge Bruker ER 042 MRH E. A Bruker ER 4116DM resonator operating in the TE 102 mode ($\nu \approx 9.5$ GHz) was used. All spectra were recorded with a modulation frequency of 100 kHz and microwave power of 2 mW with modulation amplitude of 1G. Measurements were performed with 70 mg of non-chlorinated (CeO_2-A) and 140 mg of chlorinated (CeO_2-D) samples in a quartz tube of 3 mm inner diameter. EPR spectra of both samples were collected after the following pre-treatment procedure. After degassing, the sample was heated up (10 K min^{-1}) in vacuum to the desired temperature (523, 623 and 723 K). The temperature was kept constant for 20 min, and then the sample was cooled down to room temperature. O_2 adsorption was carried out at RT by dosing 1 mbar O_2 during 5 min. Afterwards, the cell was outgassed and the sample cooled down to 77 K for collecting EPR spectra. This procedure was repeated for every treatment

temperature. Computer simulations of EPR line-shapes with Bruker Simfonia software were used to calculate spectral parameters. All spectra were normalized by the sample masses for semi-quantitative comparison of the signal double integrals after different treatments.

Results

Kinetics of chlorination and dechlorination

Previous HCl oxidation experiments over CeO_2 assessed the role of feed oxygen concentration on the stability of the catalyst.[9] It was found that no rapid deactivation occurred above a feed O_2:HCl ratio of 0.75. Post-reaction XRD measurements identified $CeCl_3 \cdot 6H_2O$ in the samples undergoing deactivation, suggesting that bulk chlorination and the corresponding phase transition induced activity loss. Furthermore, *in situ* activity restoration was possible applying high O_2 feed over-stoichiometry. Herein, using *in situ* PGAA, we evaluated the kinetics of chlorination/dechlorination of CeO_2-R under HCl oxidation conditions. Since PGAA probes the whole catalyst volume, the bulk of ceria is included in the experimentally determined Cl:Ce ratios. The BET surface area of CeO_2-R is only 5 m^2 g^{-1} (the average particle radius is ~80 nm), and, hence, the Cl:Ce ratios are small. Later we will show that Cl occupation limited to the surface of CeO_2-R gives rise to a Cl:Ce ratio of ~ 0.01 and higher numbers necessarily imply subsurface and bulk Cl contributions. It should be mentioned that by the term 'surface chlorination', we do not differentiate cus Ce occupation or surface lattice O replacement.

Three series of experiments were performed (Figure 1A). First, a reaction feed of O_2:HCl = 1:1 was set and the activity together with the Cl:Ce ratio was followed over time. Then, the oxygen content was increased stepwise leading to feeds with a O_2:HCl ratio of 2:1, 4:1, and 9:1. In the second series, directly after the first, we started with an O_2:HCl ratio of 0.5:1 and stepwise increased the oxygen content up to a ratio of 9:1. In the third series,

directly after the second, a stoichiometric (0.25:1) feed was applied and the oxygen content was again raised stepwise up to the ratio of 9:1. Figure 1B compiles the evolution of chlorine uptake and its effect on the reactivity in the three series. The first data point (1:1), taken after equilibration for 1 h, corresponds to ~ 0.02 Cl:Ce and 4% HCl conversion level. The sample continuously adsorbed chlorine, and the Cl:Ce increased up to 0.067 over the 6 h of measurement without any indication of the Cl uptake to cease. Concomitantly, the sample lost approximately 15% of its initial activity. Increasing the feed oxygen content gave rise to activity increase in line with the positive, approx. +0.5, formal order of $p(O_2)$.[9] No further rise of Cl:Ce was observed in the first set, and dechlorination was negligible in the feed of 9:1. In the second series of the experiment, strong chlorination was again evidenced at 0.5:1 and 1:1 feed ratios, and chlorination stopped at 2:1. Note, among the three series, all repeated conditions resulting in a significantly higher Cl:Ce ratio gave rise to lower HCl conversion. This time, with more than doubled Cl content, the 9:1 feed was capable to induce dechlorination with simultaneous activity recovery. Essentially similar observations could be made for the third measurement series, with the difference that the 9:1 feed enabled strong dechlorination with significant activity recovery. Note that even if dechlorination was far from complete (Cl:Ce = 0.125), the conversion level was fully restored. In fact, it was slightly even higher than in the first two series. As the whole experiment took more than 32 h, the sample at 9:1 feed worked essentially without deactivation, underlining the remarkable stability of the catalyst. Since mere surface Cl occupation leads to a Cl:Ce ratio of ~0.01, the sample under all these conditions contains much Cl below the surface. The results described suggest that (i) chlorination at low oxygen over-stoichiometry indeed gives rise to deactivation, but (ii) dechlorination at high oxygen over-stoichiometry can clean up the relevant surface sites without the necessity of removing all subsurface/bulk Cl from the material. Figure 1C depicts an example of the temporal evolution of Cl:Ce. The data

illustrates that chlorination occurs continuously with a constant rate. When analyzing the chlorination rate at 1:1 feed composition as a function of the pre-chlorination degree in the three series, only little variation was found. Thus, the chlorination rate is not much affected by the pre-chlorination degree. However, despite the continuous chlorination, no further deactivation over time was observed at 1:1 feed in the second and third series. Comparing the chlorination rate as a function of the oxygen content in the feed (Figure 1D), we found that a lower oxygen content preferentially facilitates chlorination and that sustained chlorination is absent at O_2:HCl ≥ 2. Dechlorination was not observed in the 4:1 feed, and, among the feed stoichiometries probed, only 9:1 was effective in this respect. As opposed to chlorination, dechlorination was strongly influenced by the pre-chlorination degree. Whereas almost no dechlorination was found in the first series, the estimated thickness change was -2.2 and -4.8 Å h^{-1} in the second and third series, respectively.

As chlorinated CeO_2 could be rapidly transformed back into pure CeO_2 by applying a high oxygen excess,[9] it was investigated whether rejuvenation of the oxide could be possible also starting with a pure chloride phase. Therefore, bulk $CeCl_3$ was exposed to feeds of different O_2:HCl ratio at 703 K and the used samples were analyzed by XRD (Figure 2). At O_2:HCl = 2, the HCl conversion level was very low (~ 2%) throughout the 5 h test, and only traces of cerium(IV) oxide were detected in the sample after reaction. By using the same feed composition but a 20 K higher temperature, the initially low HCl conversion progressively increased, nearly reaching the level exhibited by our reference CeO_2-A sample under identical reaction conditions (~ 22%). In this case, the original chloride phase almost fully transformed into CeO_2. Using higher feed O_2:HCl ratios (4 and 9) rapidly led to a HCl conversion level which even surpassed that expected for CeO_2 under the same conditions. The used samples were pure ceria. These data indicates that the active CeO_2 phase can be *in situ* generated from $CeCl_3$ by action of gas-phase O_2 and that the kinetics of its formation is faster for higher

oxygen excess. The overshooting of the HCl conversion values for $CeCl_3$ rejuvenated at O_2:HCl = 4 and 9 compared to CeO_2 can be partially rationalized considering that the decomposition of the chloride to produce the oxide releases Cl_2. This process is fast and complete for these samples, while slower and only partial for $CeCl_3$ exposed to lower O_2:HCl ratios. Furthermore, as the surface area of these materials is 2-3 times larger than that of CeO_2 used as reference (Table 1), they are supposed to contain a higher amount of active surface ensembles per gram of catalyst. The reaction rate per m^2 of surface after 5 h on stream is in a similar range to that of pure ceria for all rejuvenated samples, indicating a high degree of recovery of the reactivity (Table 1). Comparing this rejuvenation experiment with the dechlorination study by PGAA, the low stability of $CeCl_3$ under Deacon conditions can be clearly inferred. Subsurface Cl in O vacancy position within the oxide phase has a higher stability against dechlorination; nevertheless both dechlorination experiments revealed the same trends.

The two CeO_2 samples (CeO_2-R, CeO_2-A) investigated in this work exhibited similar intrinsic reactivity and chlorine uptake as measured by *in situ* PGAA. As we shall see in the next section, product Cl_2 inhibits the reaction, and therefore linear activity scaling by the BET surface area is not given, nevertheless the similarity of the two CeO_2 samples is still clear. Furthermore, the evolution of *in situ* Cl:Ce ratios derived as a function of reaction conditions were essentially identical, as described in the next section and shown in Figure ESI 1. Thus, the samples behave similarly in HCl oxidation.

Surface coverage analysis

Important mechanistic information may been obtained when combining different complementary *in situ* techniques[13,14,15] able to follow the changes of different adsorbed species and intermediates on the surface of the catalyst at work. As we have seen in the chlorination section, *in situ* PGAA is well suited to quantify the chlorine uptake of ceria, and

thus we can utilize the technique also to estimate the evolution of the Cl coverage as a function of the reaction conditions. One of the best complementary techniques to PGAA is *in situ* FTIR spectroscopy, affording to monitor the dynamic changes of the hydroxyl groups under reaction conditions. For the FTIR experiments, CeO_2 was activated *in situ* using synthetic air at 703 K for 90 min. After this pre-treatment, two main bands at 3700 and 3620 cm^{-1} were observed, which are assigned to mono- and doubly-coordinated hydroxyl groups, respectively.[16] These two bands vanished when introducing a mixture of O_2:HCl = 9:1 at 703 K, with the concomitant development of two signals, the main one falling at 3730 cm^{-1} and a shoulder located at 3676 cm^{-1}.[12] Furthermore, a very broad band near 3500 cm^{-1}, likely related to surface water, was also observed. Since the mono-coordinated band at 3730 cm^{-1} showed to quickly respond to changes in reactants concentrations and temperature, the integral area of this peak, obtained from fitting the absorbance spectra, was used to correlate the abundance of mono-coordinated OH groups with the catalyst reactivity under different reaction conditions. More details and spectra to the *in situ* FTIR experiments are published elsewhere.[12]

The effect of $p(O_2)$ on the concentration of OH species, referenced to the one observed in a feed of O_2:HCl = 9:1, is illustrated in Figure 3A. The amount of OH groups decreased when reducing the O_2 content in the feed, suggesting that sites to facilitate HCl adsorption need to be created by dissociative O_2 adsorption. In the case of the p(HCl) dependency (Figure 3B), the OH concentration was maximum at the lowest feed HCl concentration (1 vol.%), and steadily decreased by increasing the feed HCl content. This apparently counterintuitive result will be discussed later with the corresponding surface Cl evolution. Further, the influence of the reaction temperature on the OH concentration was also studied. It appeared that the abundance of OH progressively diminished along with temperature from 703 to 623 K (Figure 3C).

The correlation between reaction rate (mol g^{-1}_{CeO2} h^{-1}) and the abundance of OH groups on the surface for the above variation of parameters is summarized in Figure 3D. Obviously, changes in temperature and $p(O_2)$ determined the same trend, in the sense that the highest rate was achieved at the conditions (high temperature or oxygen-rich feed) that give rise to the highest OH coverage. This indicates that these two parameters may act in a similar fashion. In contrast, variation of p(HCl) revealed an opposite behavior. In fact, the highest Cl_2 productivity was achieved by using reaction conditions (high p(HCl) feed) under which the lowest surface OH concentration is observed.

Figure 4 compiles the activity data versus the Cl uptake measured by *in situ* PGAA when varying $p(O_2)$, T, p(HCl), and $p(Cl_2)$. All these experimental series started with an oxidizing treatment in pure oxygen at 723 K for 2 h. This enables to remove essentially most of the chlorine from the material. Pre-experiments indicated the effect of the studied variables on the Cl content, and thus all of these series were performed in such a way that the first measurement should induce the smallest Cl uptake and the last measurement the largest.

Figure 4A depicts the effect of $p(O_2)$. The highest oxygen containing feed (O_2:HCl = 9:1) led to the highest reactivity and to the lowest Cl uptake. Decreasing the oxygen over-stoichiometry lowered the reactivity and in parallel increased the Cl content. As shown in Figure 1B, a 1:1 feed led to a continuous increase of the chlorine content in the solid. This is seen here too, as the second measurement gave a clearly higher Cl:Ce ratio. The effect was even stronger in the 0.5:1 feed, in agreement with Figure 1D. Therefore, by decreasing the partial pressure of O_2, the Cl coverage increases slightly until the point where the chemical potential of surface Cl is high enough to induce its diffusion into the subsurface and later gives rise to a phase transition from the oxide to the chloride. Transition from purely surface to subsurface and bulk chlorination with this sample was in the Cl:Ce range of ~0.01-0.012. The effect of the temperature on the OH coverage was very similar to that of $p(O_2)$. This is

one-by-one transferable to the Cl coverage. High temperature results in higher reaction rate and concomitantly in a lower Cl content. As the *T* decreases, Cl:Ce slightly increases until at a certain temperature (653 K in this particular case) subsurface population kicks in. The trends in $p(O_2)$ and *T* can be overlaid very well, and suggest that in these experiments the Cl coverage is a key (negative) parameter governing reactivity. This simple situation however changes for the influence of *p*(HCl), as it can be deduced from Figure 4C. In a very diluted HCl-poor feed, the reactivity gets higher by increasing the inlet HCl concentration. This applies until a certain point, above which the rate drops by a further increase of *p*(HCl).[9] Note that in this experiment (Figure 4C) we only monitored the increasing activity branch. Since the O_2:HCl ratio in the $p(O_2)$ series gave rise to decreasing Cl:Ce, *p*(HCl) is expected to show an opposite behavior. This is indeed the case, as higher *p*(HCl) increases the Cl coverage. Therefore, due to the concomitant activity increase, the Cl coverage cannot be regarded *per se* as the sole negative factor reducing reactivity. Looking back at the lower OH intensity in the infrared spectra with increasing *p*(HCl), as higher *p*(HCl) will build up a higher Cl coverage, the steady-state situation should plateau at a lower OH coverage, assuming that OH recombination and water evolution are more facile than Cl_2 desorption. This likely explains the apparently counterintuitive trend in OH abundance. The situation gets even more complex when considering the effect of product co-feeding. Figure 4D shows the effect of various amounts of Cl_2 introduced into a standard feed of O_2:HCl = 9:1 on the Cl uptake. The result clearly suggests that $p(Cl_2)$ does not contribute under these oxygen-rich conditions to the Cl uptake as the Cl:Ce ratio scatters around the same ~ 0.096 value. When Cl_2 is completely switched off, no effect is observed, indicating that the Cl uptake from 5 cm^3 min^{-1} Cl_2 flow was within the error bar of the measurement. This is at odds to the inhibition experiment described in the next paragraph.

The rate of chlorine production over CeO_2-A was measured upon progressively increasing the amount of Cl_2 added to the feed mixture of O_2:HCl = 9. A negative near linear correlation was found between the reaction rate and the inlet concentration of Cl_2 added (Figure 5), indicating that molecular chlorine has a moderately strong inhibiting effect on the reactivity of the catalyst. In view of the PGAA data, this result cannot be rationalized on the basis of an increase of the surface Cl coverage in measurable quantities.

EPR experiments of O_2 adsorption

Ceria, owing to its character to reversibly exchange lattice oxygen, plays an important role in many oxidative catalytic processes. Thus, it is expected that surface chlorination influences its reducibility. Oxygen vacancies formed on the surface of the catalyst can be quantitatively investigated by means of EPR spectroscopy.[17,18,19,20] O_2 can be used as probe molecule for this purpose, because it binds to defects forming paramagnetic superoxide species, O_2^-.

EPR spectra of fresh (CeO_2-A) and chlorinated (CeO_2-D) ceria were collected, the samples being subjected to mildly reducing treatments in vacuum (~10^{-5} mbar) at different temperatures within 523-723 K followed by O_2 adsorption at 298 K, in order to form the EPR-active superoxide species. By comparing the spectra of the samples before and after chlorination, significant changes in the signals' shape and intensities were observed (Figure 6). EPR spectra of CeO_2-A show a signal with quasi-axial line shape (Figure 6A), which is assigned to superoxides species (O1-type)[21] having equivalent O atoms and lying parallel to the surface.[20] The corresponding g values are listed in Table ESI1 and agree well with the values reported in the literature. The EPR spectra of CeO_2-D exhibit a signal with a rhombic shaped (Figure 6B), with g_x shifted slightly towards higher values, which is again consistent with data found in the literature for a chlorinated sample.[22] As opposed to g_x, the g_y and g_z values are essentially unaffected upon chlorination. Note that according to the so-called

ionic model of the M^{n+}-O_2^- radicals, the g_x tensor value must lie very close to the free electron g value (g_e = 2.0023), bearing in mind that the x axis is considered to be normal to the O-O-M^{n+} plane.[23] Thus, a plausible interpretation of the g_x shift is a somewhat higher degree of covalent character in the Ce^{4+}-O_2^- bond induced by the substitution of lattice O atoms by Cl.[24]

The amount of paramagnetic species produced on the samples was obtained from the double integration of the signals. Figure 6C shows that a maximum amount of superoxide species was formed over CeO_2-A as a function of the reduction temperature and that outgassing at higher temperature gave rise to a decline of the superoxide intensity. Intuitively, one would expect even more reduced sites at higher temperature, and hence the formation of more superoxide species. However, at high temperatures oxygen vacancies can diffuse into the bulk, since this is energetically more favored compared to being trapped at the surface,[25] and, thus, less superoxide could form. Additionally, at higher *T* vacancies may cluster and upon O_2 adsorption these can be filled by O_2 dissociation, thus impeding the formation of superoxides. The chlorinated sample generally produced fewer superoxide species, and exhibited a much smaller effect on temperature changes. No maximum was found in this case, and the highest superoxide signal intensity was observed after pre-treatment at 723 K. Hence, we can conclude that chlorination inhibits facile vacancy formation and, thus, lowers the propensity of ceria to activate oxygen.

Discussion

A relatively simple catalytic reaction, HCl oxidation over CeO_2, has been investigated, and we focused our attention 1) on the chemical changes occurring on the surface and in the near-surface region of ceria, and 2) to quantify the surface species under multiple steady states; with the hope to correlate both 1) and 2) with reactivity. PGAA experiments following chlorination and dechlorination kinetics have clearly indicated the detrimental role of

subsurface/bulk chlorination on the reactivity. It is likely that this has its origin in the high surface Cl coverage necessary for facilitating Cl diffusion into the bulk and concomitant removal of lattice O in the formation of water. Losing lattice O/vacancy dynamics by extended near-surface chlorination hinders oxygen activation. EPR experiments have shown that the number of surface O vacancies enabling the formation of superoxide species upon O_2 adsorption drastically diminishes for the chlorinated sample. This implies that oxygen activation during HCl oxidation is a critical elementary step when the Cl surface coverage is high. Our recent characterization of the acid/base properties of ceria after HCl oxidation indicated that sites with basic character were essentially eliminated from the surface of chlorinated CeO_2.[12] That is, most of the lattice O sites have been exchanged by Cl and the OH groups formed are rather acidic. Notice, HCl activation is thought to require basic sites to abstract H. Therefore, it is not surprising to see that $p(O_2)$ has a clear negative effect on the Cl uptake and a concomitant positive influence on reactivity. Higher O_2 over-stoichiometry will liberate chlorinated sites by dissociative O_2 adsorption to enable HCl dissociative adsorption. This gives rise to less site blocking by Cl and a higher population of OH groups.

Remarkably, Cl and OH population changes were, as a rule, complementary upon variation by the reaction conditions ($p(O_2)$, p(HCl), and T). Higher temperature and $p(O_2)$ as well as lower p(HCl) decreased Cl and increased OH coverage. This indicates that the major role of temperature is to diminish site blocking by Cl. On the contrary, increasing p(HCl) gives rise to higher Cl coverage and parallel increase of reactivity, though only in the range where no subsurface and bulk chlorination sets in. This influence of HCl partial pressure points to a significantly more complex role of the coverage with Cl containing species, which may be divided into two contributions: one major part being detrimental, as discussed, most probably by site blocking, whereas a small but certain part is “reactive”. Surface sites binding Cl after dissociation less strongly can contribute to the latter group. Further, during HCl

oxidation lateral interactions at high coverages may give rise to lower heat of adsorption of reactants that can accelerate the reaction. Such lateral interactions for adsorbed HCl may be operative in increasing reactivity at high HCl partial pressures.

Molecular chlorine was predicted to have a weak effect on surface chlorination.[9] Only at high $p(Cl_2)$ and very low $p(O_2)$ surface Cl will stabilize in a lattice O vacancy or at the cus Ce^{4+} site. This is in perfect agreement with our PGAA observation, as extra Cl_2 product co-feeding in the range investigated (up to 5 cm^3 STP min^{-1} Cl_2 next to 16.6 cm^3 STP min^{-1} HCl) was not able to induce any increase of the Cl:Ce ratio. On the other hand, Cl_2 gives rise to strong inhibition, as the same amount (5 cm^3 STP min^{-1}) of Cl_2 reduced reactivity by ~45%. The way products can inhibit reaction is most often related to site blocking by adsorption. Further, the heat of adsorption of reactants may be modulated by other adsorbates (promoters and poisons), but interaction of Cl_2 with ceria is weak and dissociation leads to surface Cl, hence inhibition by the modification of the surface electronic structure is not likely. Since Cl_2 inhibition is not persistent and turning off Cl_2 product feeding restores reactivity quickly, complex restructuring phenomena are also not likely, and rather inhibition is expected to occur by competitive adsorption and site blocking. As, however, this was not observable within the uncertainty (~2%) of the experiment, one can conclude that the number of sites critically involved in the reaction should be very small (also in the range of few percent). Consequently, most surface sites probed in the *in situ* spectroscopic (FTIR and PGAA) experiments correspond to either sites holding spectators, or function only as buffer. The reactivity of most surface sites is thus likely negligibly low and only very few high energy sites can effectively contribute in the observed catalytic turnover. Nevertheless, nearby sites temporarily storing surface species may supply adsorbates to the high energy site, which may effectively catalyze recombination and desorption of products. Then, the convincing correlations found in the *in situ* FTIR and PGAA experiments (Figures 3 and 4) do *not*

correspond to the relevant active surface sites, but rather describe the equilibration of the major non-reactive surface units with the reactants and the adjustment to the reaction conditions. Although *in situ* or *operando* studies deserve the attention of the catalysis community and usually represent a step up from standard works with reactivity and *ex situ* characterization, the experiments described here suggest that one should at least exercise some caution when deriving strong conclusions from a limited set of *in situ* (*operando*) experiments. Investigating a larger set of variables may override frivolously derived correlations and conclusions.

Conclusions

Ceria is a catalyst with high industrialization potential for HCl oxidation. We have investigated various aspects of this reaction system. Subsurface and bulk chlorination gives rise to deactivation, and we studied the kinetics of this as well as the inverse dechlorination process. In line with the negative role of chlorination, the rate of chlorination is higher with lower oxygen over-stoichiometry (but is independent of the pre-chlorination degree), whereas dechlorination is facilitated at high oxygen partial pressures. At the limit, $CeCl_3$ transforms to CeO_2 under reaction condition.

The surface coverage of the two most abundant species Cl and OH was followed under multiple steady states as a function of $p(O_2)$, $p(HCl)$, $p(Cl_2)$, and T without the influence of subsurface chlorination. Oxygen and temperature removes some surface Cl and increases the OH population with concomitant reactivity enhancement. Hence, in these experiments OH positively and Cl negatively correlates with the reactivity. On the other hand, in oxygen-rich feeds higher $p(HCl)$ gives rise to increased activity, but also to higher coverage of Cl containing species (and less OH), and, therefore, here an opposite trend is observed. Lastly, Cl_2 strongly inhibits the reaction but no measureable increase of Cl uptake

was found. This latter result leads us to the conclusion that essentially all of the surface probed in the *in situ* experiments correspond to the main part of the surface bearing little relevance to the reactivity. This complex set of experiments highlights the role to investigate a broad field of reaction parameters before deriving strong but artificial surface-reactivity correlations.

Acknowledgement

The authors acknowledge support from BMBF Project 033R018A, Bayer MaterialScience, ETH Zurich, the EU FP7 NMI3 Access Programme, the NAP VENEUS grant (OMFB-00184/2006) and the cooperation project between the Fritz-Haber Institute and the former Institute of Isotopes funded by the MPG. Bayer MaterialScience is acknowledged for permission to publish this article. Núria López is thanked for valuable discussions.

Figures

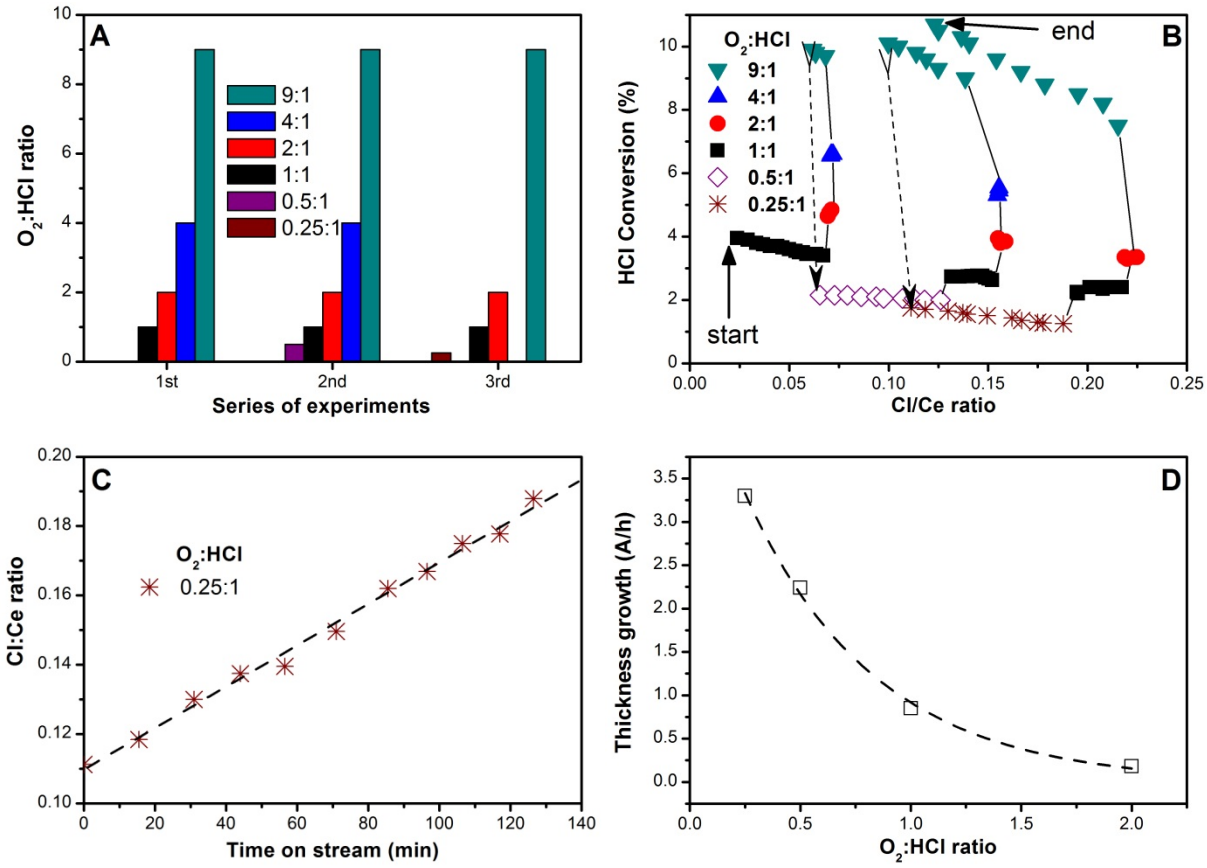

Figure 1: Series of chlorination/dechlorination experiments over CeO_2-R at 703 K by *in situ* PGAA. A) Map of experiments with three series. Various O_2:HCl feed ratios (10% HCl, 2.5-90% O_2 balanced in N_2) were probed. Measurements were performed from left to right consecutively, however for different time periods. B) Evolution of HCl conversion and Cl uptake (as Cl:Ce) in the experiments. The first data point is at 4% conversion. The lines guide the eyes to follow the order of experiments. C) An example of Cl uptake over time-on-stream with a feed of O_2:HCl = 0.25:1. D) Thickness growth of chlorinated shell as a function of the feed oxygen content. The rate of Cl uptake was evaluated in a simple geometric model (with particle radius of 82 nm) and assuming a homogeneous growth of the chlorinated surface shell towards the particle core. The thickness growth describes the speed of the chlorinated front moving toward the core of the ceria particle.

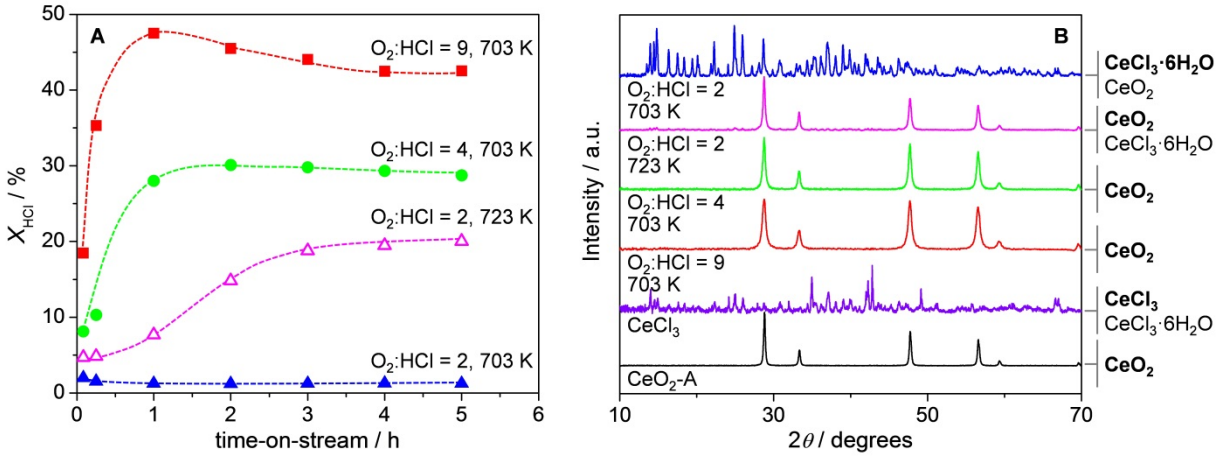

Figure 2: Rejuvenation of the CeO_2 phase from $CeCl_3$ under Deacon conditions. (A) HCl conversion *versus* time-on-stream over $CeCl_3$ at various O_2:HCl ratios and temperatures. Other conditions: 10 vol.% HCl and 20-90 vol.% O_2 balanced in N_2, space time = 11.2 g h mol^{-1}, total volumetric flow = 166 cm^3 STP min^{-1}, and 1 bar. (B) XRD patterns of fresh CeO_2-A, fresh $CeCl_3$, and $CeCl_3$ samples resulted from the catalytic tests. The right panel lists the crystalline phases present in the samples, with the predominant phase in bold: CeO_2 (JCPDS 73-6328), $CeCl_3$ (JCPDS 77-0154), $CeCl_3 \cdot 6H_2O$ (JCPDS 01-0149).

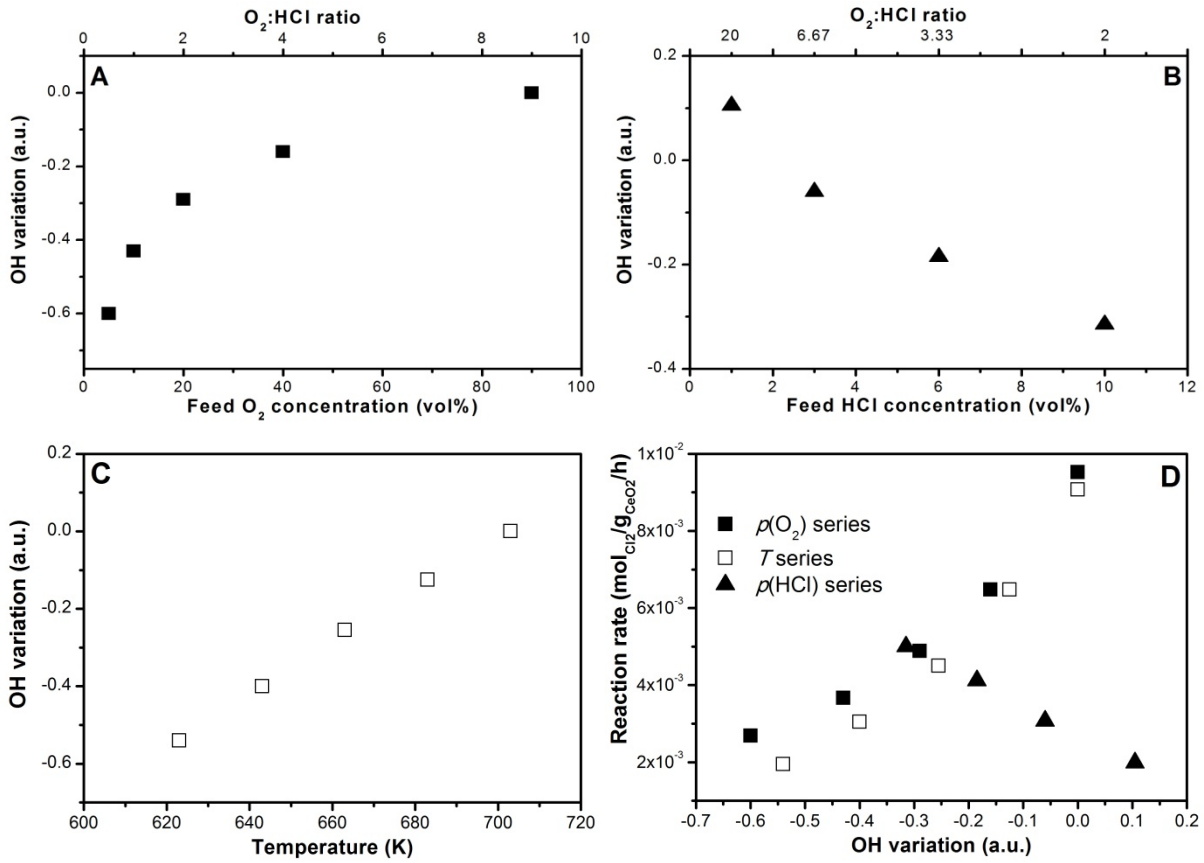

Figure 3: Evolution of the intensity of the mono-coordinated OH band at 3730 cm^{-1} as a function of (A) $p(O_2)$, (B) p(HCl), (C) temperature as measured by *in situ* FTIR on CeO_2-A. The absorbance spectra were fitted and the area variation referenced to the condition O_2:HCl = 9:1 at 703 K was plotted. D) Reaction rate, measured in parallel by iodometric titration, versus the intensity of the OH band under different conditions.

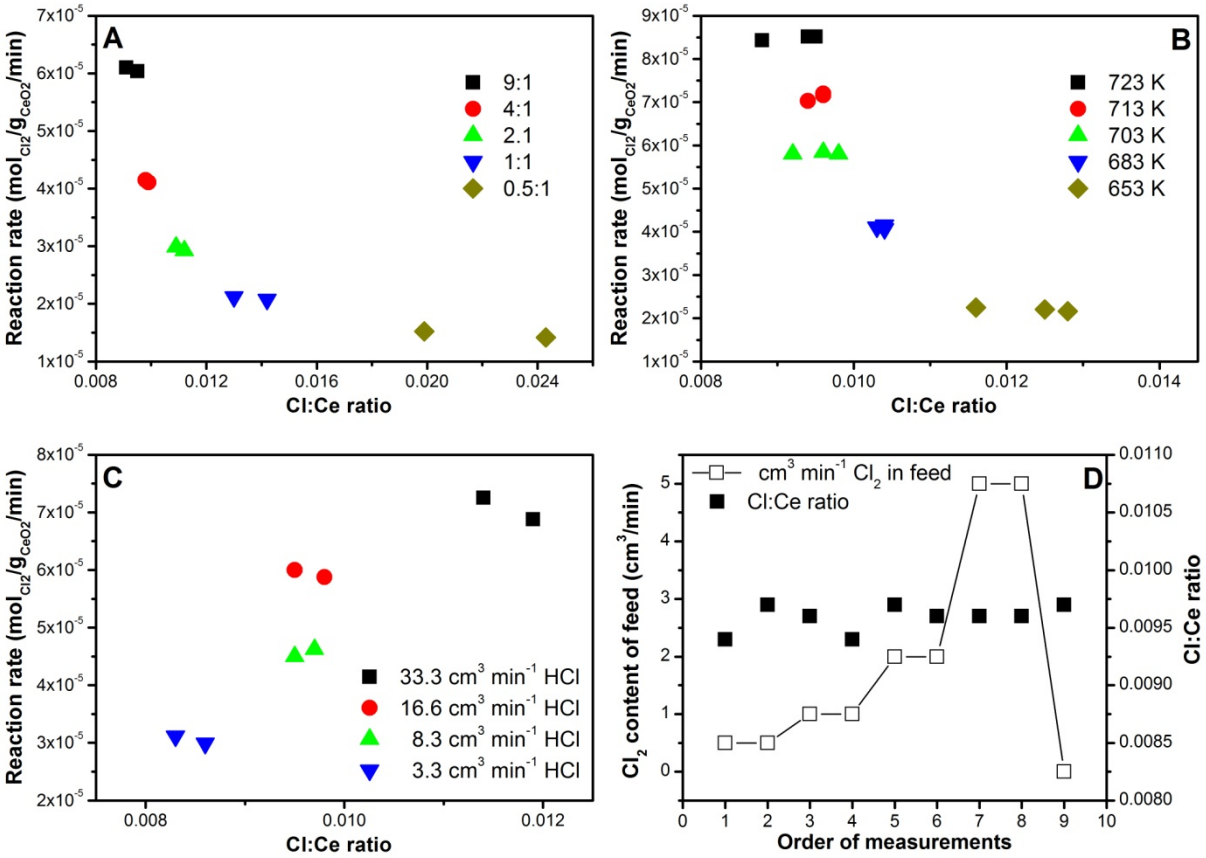

Figure 4: *In situ* PGAA experiments on CeO_2-R showing the reaction rate evolution as a function of Cl:Ce ratio under various conditions. In (A) the feed oxygen content (at 703 K), in (B) the temperature (at O_2:HCl = 9:1) and in (C) the feed HCl content (at 703 K) was varied. (D) Cl:Ce ratio as a function of various amounts of Cl_2 co-dosed to a 9:1 feed at 703 K. In ESI, corresponding $p(O_2)$ and T dependences on CeO_2-A are shown to be identical to those given here. Table 1 suggests that with CeO_2-R and CeO_2-A both reactivity and Cl uptake are similar when normalized to the corresponding BET surface area.

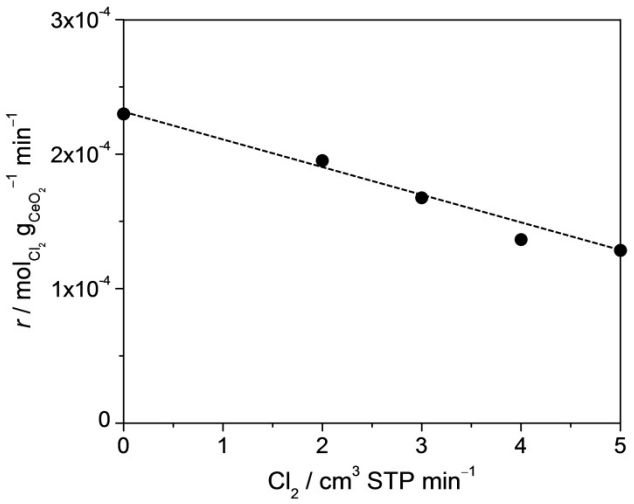

Figure 5: Influence of Cl_2 co-feeding on the rate of HCl oxidation over CeO_2-A. Conditions: 10 vol.% HCl and 90 vol.% O_2, 703 K, space time = 5.6 g h mol^{-1}, total volumetric flow = 166 cm^3 STP min^{-1}, 1 bar, and dwelling time under each condition = 1.5 h.

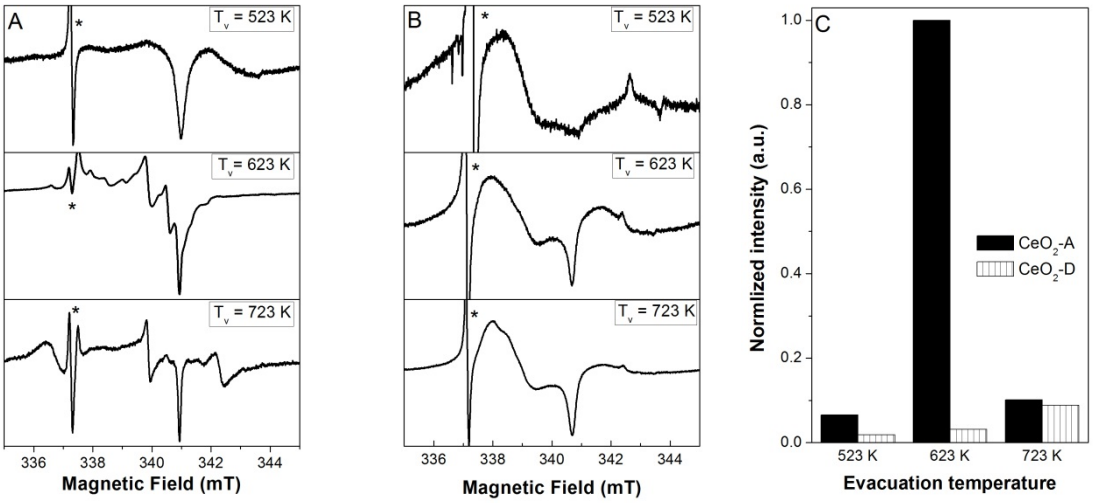

Figure 6: EPR signals of superoxide species produced by O_2 adsorbed at RT on pre-reduced samples (A) CeO_2-A and (B) CeO_2-D. Signal marked with * is due to highly EPR-active Mn^{2+} impurities in the ceria. (C) The amount of superoxide was quantified by double integration of signals assigned to superoxides.

References

[1] M. M. Schubert, M. J. Kahlich, H. A. Gasteiger, R. J. Behm, J. Power Sources 84, 1999, 175.

[2] L. J. Burcham, L. E. Briand, I. E. Wachs, Langmuir 17, 2001, 6174.

[3] F. C. Meunier, Catal. Today 155, 2010, 164.

[4] T. Hibi, H. Abekawa, K. Seki, T. Suzuki, T. Suzuta, K. Iwanaga, T. Oizumi, EP936184, 1999.

[5] A. Wolf, L. Mleczko, O. F. Schlüter, S. Schubert, EP2026905, 2006.

[6] J. Pérez-Ramírez, C. Mondelli, T. Schmidt, O. F. -K. Schluter, A. Wolf, L. Mleczko, T. Dreier, Energy Environ. Sci. 4, 2011, 4786.

[7] H. Over, J. Phys. Chem. C 116, 2012, 6779.

[8] D. Teschner, R. Farra, L.-D. Yao, R. Schlögl, H. Soerijanto, R. Schomaecker, T. Schmidt, L. Szentmiklósi, A.P. Amrute, C. Mondelli, J. Pérez-Ramírez, G. Novell-Leruth, N. López, J. Catal. 285, 2012, 273.

[9] A. P. Amrute, C. Mondelli, M. Moser, G. Novell-Leruth, N. Lopez, D. Rosenthal, R. Farra, M. E. Schuster, D. Teschner, T. Schmidt, J. Pérez-Ramírez, J. Catal. 286, 2012, 287.

[10] Zs. Révay, T. Belgya, L. Szentmiklósi, Z. Kis, A. Wootsch, D. Teschner, M. Swoboda, R. Schlögl, J. Borsodi, R. Zepernick, Anal. Chem. 80, 2008, 6066.

[11] A.P. Amrute, C. Mondelli, J. Pérez-Ramírez, Catal. Sci. Tech. 2, 2012, 2057.

[12] R. Farra, M. E. Schuster, S. Wrabetz, E. Stotz, N. G. Hamilton, A. P. Amrute, J. Pérez-Ramírez, N. López, D. Teschner, Phys. Chem. Chem. Phys., submitted

[13] X. T. Gao, S. R. Bare, J. L. G. Fierro, M. A. Banares, I. E. Wachs, J. Phys. Chem. B 102, 1998, 5653.

[14] L. Burcham, G. Deo, X. Gao, I. Wachs, Top. Catal. 11-12, 2000, 85.

[15] G. Le Bourdon, F. Adar, M. Moreau, S. Morel, J. Reffner, A. S. Mamede, C. Dujardin, E. Payen, Phys. Chem. Chem. Phys. 5, 2003, 4441.

[16] A. Badri, C. Binet, J.-C. Lavalley, Faraday Trans. 92, 1996, 4669.

[17] M. Gideoni, M. Steinberg, J. Solid State Chem. 4, 1972, 370.

[18] A. Aboukais, E. A. Zhilinskaya, J.-F. Lamonier, I. N. Filimonov, Colloids Surf., A 260, 2005, 199.

[19] M. Che, J. F. J. Kibblewhite, A. J. Tench, M. Dufaux, C. Naccache, J. Chem. Soc., Faraday Trans. 1 69, 1973, 857.

[20] A. Martínez-Arias, J. C. Conesa, J. Soria, Res. Chem. Intermed. 33, 2007, 775.

[21] J. Soria, A. Martínez-Arias, J. C. Conesa, Faraday Trans. 91, 1995, 1669.

[22] J. Soria, J. C. Conesa, A. Martínez-Arias, Colloids Surf., A 158, 1999, 67.

[23] M. Anpo, M. Che, B. Fubini, E. Garrone, E. Giamello, M. Paganini, Top. Catal. 8, 1999, 189.

[24] J. Soria, A. Martínez-Arias, J. M. Coronado, J. C. Conesa, Top. Catal. 11-12, 2000, 205.

[25] M. V. Ganduglia-Pirovano, J. L. F. Da Silva, J. Sauer, Phys. Rev. Lett. 102, 2009, 026101.